Research Square

Preprints are preliminary reports that have not undergone peer review.
They should not be considered conclusive, used to inform clinical practice,
or referenced by the media as validated information.

Closed-Form Residence-Time Modelling of Swirling Waste-Gas Injection Using the Lambert-W Function: Benchmarking Against Published CFD Data

MohammadReza Modarres

mohammad@adai.pt

Associação para o Desenvolvimento da Aerodinâmica Industrial

Research Article

Keywords: esidence time, residence-time distribution, swirling flow, Lambert W function, reduced order modelling, waste-gas incineration, turbulent momentum relaxation, CFD benchmark

Posted Date: October 27th, 2026

DOI: https://doi.org/10.21203/rs.3.rs-11210983/v1

License: This work is licensed under a Creative Commons Attribution 4.0 International License.
Read Full License

Additional Declarations: No competing interests reported.

Closed-Form Residence-Time Modelling of Swirling Waste-Gas Injection Using the Lambert–W Function: Benchmarking Against Published CFD Data

MohammadReza Modarres*

ADAI, Department of Mechanical Engineering, Universidade de Coimbra

Rua Luís Reis Santos, Pólo II, 3030-788 Coimbra, Portugal

mohammad@adai.pt

*Corresponding author: MohammadReza Modarres, mohammad@adai.pt

Abstract

Residence time is a key quantity governing mixing, conversion and pollutant exposure in swirling combustion systems. Three-dimensional computational fluid dynamics (CFD) can resolve the resulting non-uniform trajectories, but the physical dependence of transit time on inlet momentum and turbulent relaxation is less transparent in a reduced-order description. This work develops a closed-form axial residence-time model in which an injected fluid element relaxes toward a representative bulk axial velocity through a single Lagrangian time scale. The governing trajectory equation is inverted exactly with the Lambert-W function. The solution is controlled by two dimensionless groups, the inlet-to-bulk velocity ratio $\Theta = w_0/\bar{w}$ and the relaxation parameter $\Lambda = \bar{w}T_L/H$.

The analytical formulation is benchmarked against the complete residence-time dataset reported by Darbandi et al. for a swirl-assisted waste-gas incinerator. The published residence-time curves for the original main scheme and for circular, square and rectangular waste-gas inlet cross-sections are reconstructed from the published residence-time figure of the original paper. At an incinerator height of 8 m, the reconstructed residence times are 0.93 s, 1.37 s, 1.35 s, and 0.90 s for the main, circular, square and rectangular configurations, respectively. Thus, the circular and square configurations produce residence times approximately 47% and 45% greater than the main scheme, whereas the rectangular configuration is approximately 3% lower. The corresponding cumulative transit velocities, H/τ, are approximately 8.6 m/s, 5.8 m/s, 5.9 m/s, and 8.9 m/s. The strong curvature of the reconstructed trajectories and their dependence on inlet cross-section demonstrate that a single axial relaxation mechanism cannot, by itself, represent the geometry-dependent transport observed in the three-dimensional CFD.

The reduced-order solution is therefore used as an analytical reference rather than as a replacement for CFD. Its principal value is to separate the contribution of axial momentum relaxation from the additional residence-time effects associated with swirl, recirculation and geometry-dependent redistribution. Experimental and large-eddy-simulation studies of confined swirling flows provide independent support for this interpretation by showing that non-ideal residence-time distributions arise from multiple transport zones and recirculation structures.

Keywords: Residence time; residence-time distribution; swirling flow; Lambert W function; reduced-order modelling; waste-gas incineration; turbulent momentum relaxation; CFD benchmark

1 Introduction

Residence time is a fundamental descriptor of transport in combustion and chemical reactors because it determines the duration available for mixing, reaction and species transformation. In practical combustion systems, however, a single hydraulic residence time is often insufficient. Spatially separated recirculation zones, preferential transport paths and turbulent dispersion produce a distribution of transit times rather than a unique value. Experimental measurements in confined swirling flows have consequently been interpreted using combinations of plug-flow and continuously stirred regions rather than a single ideal-reactor description [2]. Large-eddy simulations (LES) of complex swirling combustion chambers likewise show non-ideal residence-time distributions and finite higher-order moments [3].

Swirling flow is particularly relevant to waste-gas incineration because angular momentum modifies entrainment, mixing and the persistence of recirculating structures. The resulting residence time depends not only on the axial flow rate but also on the way the inlet momentum is introduced into the chamber. The effect of inlet geometry is therefore an important problem for reduced-order modelling.

Darbandi et al. [1] investigated a waste-gas incinerator using three-dimensional CFD and Lagrangian particle tracking. Their study compared the original main configuration with three modified waste-gas inlet cross-sections—circular, square and rectangular—for tangentially and upward-directed inlet streams. The authors reported substantial differences in both mixing behavior and species residence time. In particular, the residence-time curves in the corresponding figure of that paper (numbered Fig. 22 in Ref. [1]; it is not part of the present manuscript and is redrawn from digitized data as Fig. 3) show that the modified inlet geometries do not simply produce a constant shift in transit time; the curvature of the trajectories changes with height and the relative ordering of the configurations is not constant over the full chamber.

The study of Darbandi et al. [1] provides a suitable benchmark for the present work because it reports residence-time results for multiple inlet geometries obtained using a consistent CFD framework and

Lagrangian particle tracking methodology. The present paper develops a new analytical interpretation and re-analysis of the published results.

These results provide a benchmark for evaluating reduced-order transport formulations. The objective of the present work is not to replace CFD, but to isolate the contribution of axial momentum relaxation from the additional transport mechanisms associated with swirl-induced recirculation, three-dimensional redistribution, and geometry-dependent residence-time enhancement. By providing an exact baseline for momentum relaxation along the main flow direction, this formulation establishes a physical standard against which the impact of complex 3D flow structures and turbulent mixing dynamics can be directly isolated and quantified.

The present work develops an exact one-dimensional residence-time solution and applies it to the complete Darbandi dataset rather than selecting a single inlet configuration. The objectives are:

1. to derive a closed-form expression for the transit time of a fluid element subject to first-order axial velocity relaxation;
2. to identify the dimensionless parameters controlling the analytical solution and its limiting behavior;
3. to reconstruct and analyze the full residence-time dataset reported for the main, circular, square and rectangular Darbandi configurations;
4. to quantify the geometry-dependent residence-time enhancement using cumulative transit velocity and constant-velocity reference measures;
5. to establish the appropriate interpretation and limitations of the analytical model using independent experimental and LES literature on swirling flows.

2 Darbandi benchmark and reconstruction of the published CFD data

2.1 Original CFD study

Darbandi et al. [1] performed a cold-gas CFD analysis of an industrial waste-gas incinerator. The simulations used a three-dimensional unstructured mesh, a standard k–ε turbulence model, and Lagrangian particle tracking for the residence-time calculation. The inlet study considered the original main scheme and three modified waste-gas configurations with circular, square and rectangular cross-sections. The modified streams were introduced tangentially and with an upward inclination of approximately 45°.

The inlet data reported by Darbandi et al. include a waste-gas temperature of 338.15 K, a mass flow rate of 2084 g/s, a hydraulic diameter of 350 mm, and an inlet pressure of approximately 82 kPa. The air

and fuel-gas streams were also included in the CFD solution. Using the reported temperatures, pressures, compositions and mass flow rates with an ideal-gas calculation gives a total inlet volumetric flow of approximately

$$Q \simeq 5.28\,\mathrm{m}^3/\mathrm{s}. \tag{1}$$

This value is useful for establishing the order of magnitude of the system throughput, but it is not used as an independent determination of the axial velocity in the residence-time benchmark because the published paper does not provide a sufficiently complete height-dependent cross-sectional velocity field for that purpose.

2.2 Reconstruction of the published residence-time curves

The residence-time data were reconstructed from the published curves in the residence-time figure of Darbandi et al. [1] (Fig. 22 of that paper, not of the present manuscript); the reconstruction is shown in Fig. 3. This procedure does not represent a new CFD calculation. It is a numerical reconstruction of the published graphical results because the underlying Lagrangian data were not supplied in tabulated form.

The complete set of four configurations was retained:

1. Main Scheme;
2. Waste Gas with Circular Cross Section;
3. Waste Gas with Rectangular Cross Section;
4. Waste Gas with Square Cross Section.

The plotted markers and connecting curves were digitized in the residence-time–height coordinate system. The reconstructed data were then smoothed only for graphical interpolation and cumulative quantities; the reported benchmark values are rounded to three decimal places and should be regarded as approximate values recovered from the published figure rather than as original tabulated CFD output.

Table 1 reports the reconstructed residence times at integer heights. The values reported elsewhere in this paper are obtained from the complete reconstructed dataset and therefore may differ slightly from the rounded values listed in Table 1. The complete digitized working dataset is distributed with the accompanying Python script at 0.25 m intervals.

The reconstructed curves reproduce two features that are central to the present analysis. First, the main and rectangular configurations remain comparatively close. Second, the circular and square configurations develop substantially larger residence times, particularly after approximately 2 m–3 m, and the slopes of

Table 1: Residence times reconstructed from the residence-time figure of Darbandi et al. [1]. Values are rounded to 0.001 s; they are graphical reconstructions rather than original tabulated CFD data.

Height H (m)	Main (s)	Circular (s)	Rectangular (s)	Square (s)
1	0.043	0.043	0.056	0.035
2	0.107	0.114	0.116	0.093
3	0.164	0.350	0.190	0.240
4	0.245	0.633	0.283	0.461
5	0.395	0.967	0.419	0.661
6	0.651	1.109	0.614	0.939
7	0.780	1.206	0.760	1.125
8	0.903	1.318	0.866	1.308

their curves change markedly with height. These features cannot be represented by replacing the complete curves with a single residence-time value.

3 Reduced-order residence-time formulation

3.1 Axial relaxation model

Consider a fluid element entering a reactor at $z = z_{\mathrm{in}}$ with axial velocity w_0. The representative axial velocity of the surrounding bulk flow is denoted by $\bar{w}$. The reduced-order model assumes

$$\frac{\mathrm{d}w}{\mathrm{d}t} = -\frac{w - \bar{w}}{T_L}, \qquad \frac{\mathrm{d}z}{\mathrm{d}t} = w, \tag{2}$$

where T_L is an effective Lagrangian momentum-relaxation time.

The model deliberately treats T_L as an effective parameter. In a detailed turbulence model it may be related to local turbulent kinetic energy and dissipation, for example through a relation of the form $T_L = C_L k/\varepsilon$, but no universal value of C_L is assumed here. This distinction is important because the Darbandi publication does not provide the full three-dimensional k and ε fields required to evaluate such a relation along every Lagrangian trajectory.

The initial axial velocity is written as

$$w_0 = \Theta \bar{w}, \tag{3}$$

where Θ is the inlet-to-bulk axial velocity ratio.

For constant $\bar{w}$, Eq. (2) gives

$$w(t) = \bar{w} + (w_0 - \bar{w}) \exp\left(-\frac{t}{T_L}\right). \tag{4}$$

Integration of the axial velocity gives

$$H = \bar{w}t + (w_0 - \bar{w})T_L\left(1 - \exp\left[-\frac{t}{T_L}\right]\right), \tag{5}$$

where $H = z - z_{\text{in}}$.

3.2 Exact Lambert-W inversion

Define

$$a = \Theta - 1, \qquad x = \frac{H}{\bar{w}T_L}. \tag{6}$$

Equation (5) can be written as

$$x = y + a - ae^{-y}, \qquad y = \frac{t}{T_L}. \tag{7}$$

Rearrangement gives

$$(y + a - x)e^{y+a-x} = ae^{a-x}. \tag{8}$$

Therefore, the exact residence time is

$$\boxed{\tau(H) = \frac{H}{\bar{w}} - aT_L + T_L W_0\left(a\exp\left[a - \frac{H}{\bar{w}T_L}\right]\right)} \tag{9}$$

where W_0 denotes the principal branch of the Lambert-W function.

The expression satisfies $\tau(0) = 0$ and remains real for all physically relevant $\Theta > 0$ on the principal branch. Equation (9) is the central analytical result of the paper.

3.3 Dimensionless form

Introducing

$$\Theta = \frac{w_0}{\bar{w}}, \qquad \Lambda = \frac{\bar{w}T_L}{H}, \tag{10}$$

gives

$$\boxed{\frac{\tau\bar{w}}{H} = 1 - (\Theta - 1)\Lambda + \Lambda W_0\left[(\Theta - 1)\exp\left(\Theta - 1 - \frac{1}{\Lambda}\right)\right].} \tag{11}$$

The dimensionless solution is plotted in Fig. 1.

The two limits provide useful physical checks. For rapid relaxation,

$$\Lambda \to 0: \qquad \tau \simeq \frac{H}{\bar{w}} + (1 - \Theta)T_L. \tag{12}$$

For negligible relaxation,

$$\Lambda \to \infty : \qquad \tau \to \frac{H}{w_0} = \frac{H}{\Theta \bar{w}}. \tag{13}$$

For matched inlet and bulk velocity,

$$\Theta = 1 : \qquad \tau = \frac{H}{\bar{w}}. \tag{14}$$

4 Independent verification of the analytical solution

The closed-form expression was independently verified by integrating Eq. (2) with adaptive Runge–Kutta time integration and terminating the integration when $z = H$. A logarithmic grid covering $0.2 \leq \Theta \leq 8$ and $0.01 \leq \Lambda \leq 100$ was used for the verification.

Across the tested parameter grid, the maximum relative difference between the Lambert-W solution and the numerical event-detected integration was below 3×10^{-12} when tight integration tolerances were applied. This verifies the algebraic inversion independently of the Darbandi CFD benchmark; the residual differences are shown in Fig. 2.

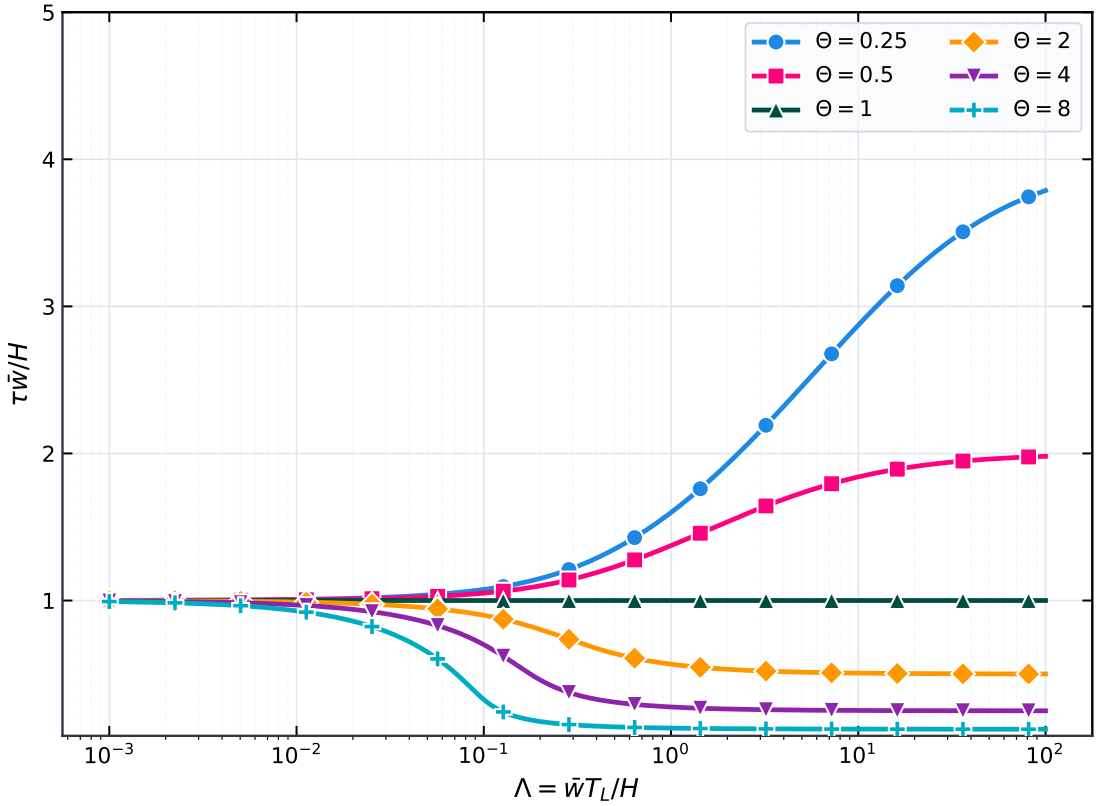

Figure 1: Dimensionless residence-time solution, $\tau\bar{w}/H$, from the exact Lambert-W expression. The independent parameters are the inlet-to-bulk axial velocity ratio Θ and the relaxation parameter $\Lambda = \bar{w}T_L/H$.

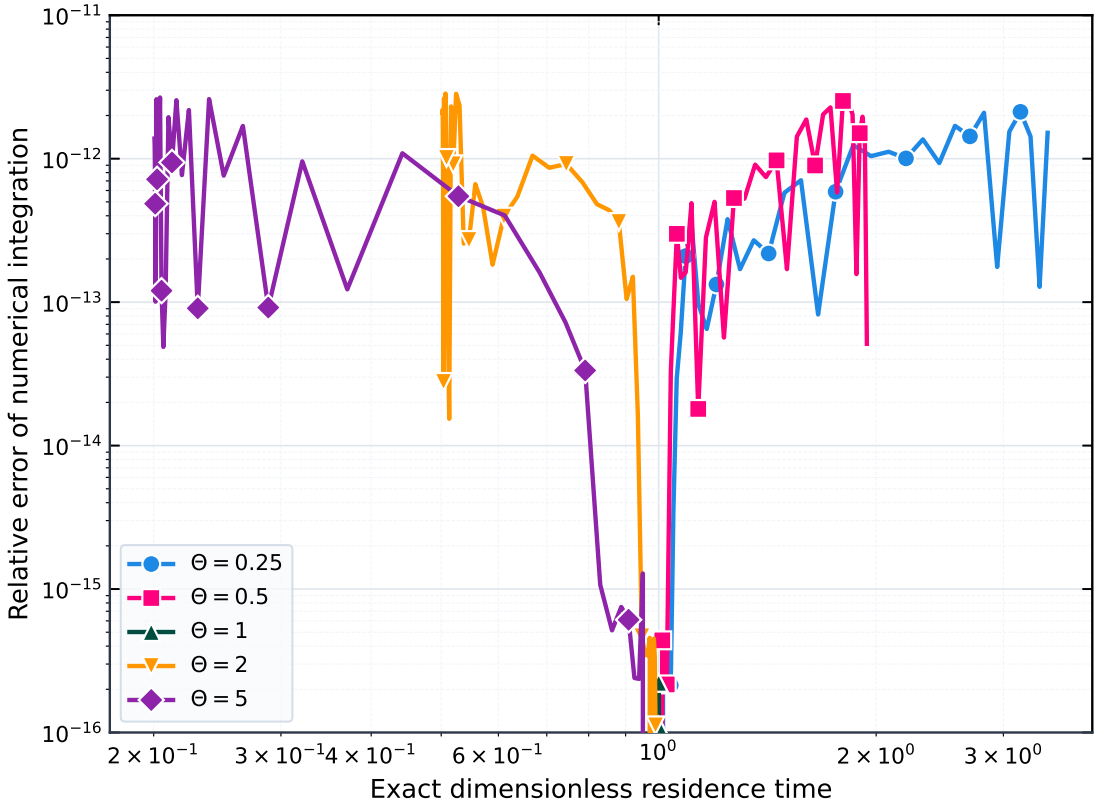

Figure 2: Verification of the closed-form Lambert-W solution against adaptive numerical integration of the governing axial relaxation equations.

5 Full analysis of the Darbandi residence-time dataset

5.1 Residence-time evolution

Figure 3 shows the complete reconstructed residence-time curves. The four configurations do not collapse onto a single linear relation of the form $\tau = H/U$. Instead, each curve changes slope with height.

The main and rectangular configurations remain comparatively close. At the upper part of the furnace their residence times are approximately 0.93 s and 0.90 s, respectively. In contrast, the circular and square configurations reach approximately 1.37 s and 1.35 s. Relative to the main scheme, these correspond to increases of approximately 47% and 45%, respectively, whereas the rectangular configuration is approximately 3% lower.

More significant than the terminal residence time is the progressive divergence of the curves with increasing height. The geometry-dependent divergence begins within the chamber and develops progressively with height. A single correction factor applied to a hydraulic transit time would therefore be insufficient to represent the complete curves.

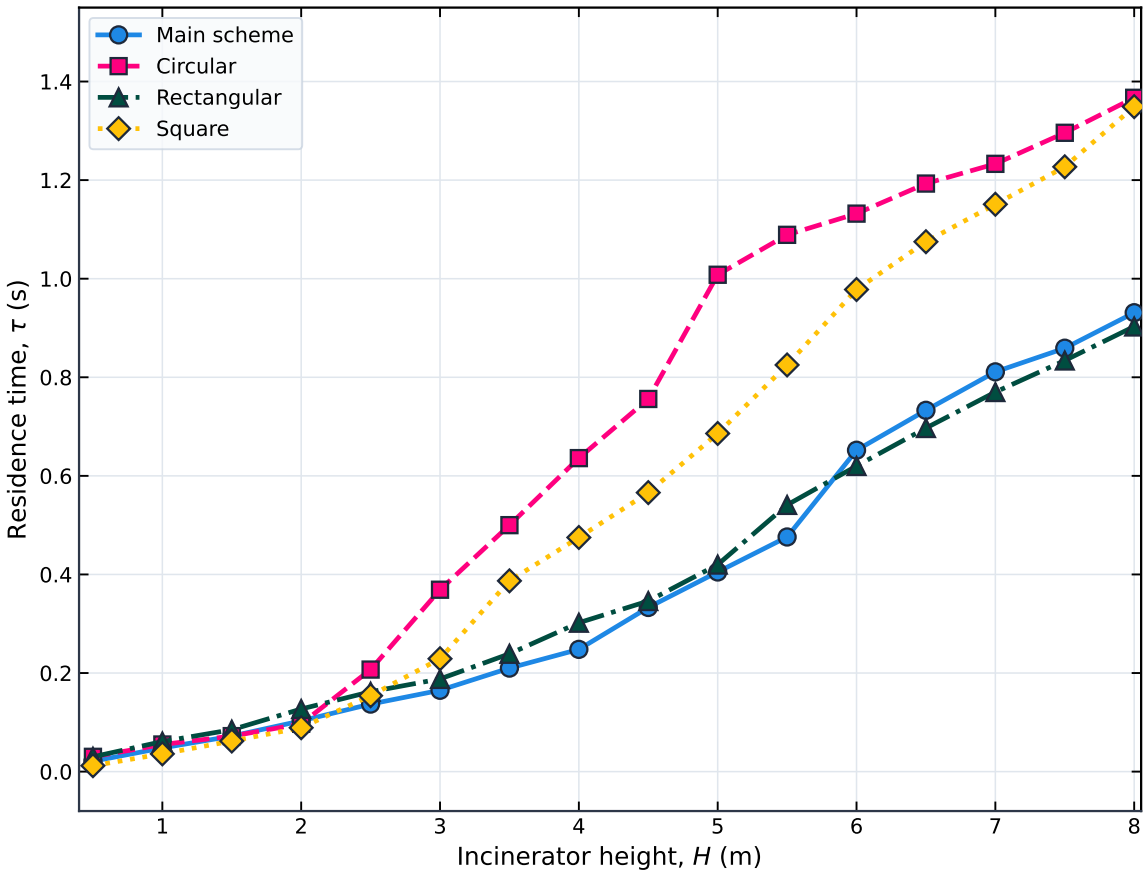

Figure 3: Complete reconstruction of the residence-time curves reported in the residence-time figure of Darbandi et al. [1] (Fig. 22 of that paper). All four published configurations are retained: main scheme, circular, rectangular and square waste-gas inlet cross-sections. Markers represent the digitized working dataset and lines are smooth interpolations used only for visualization.

5.2 Cumulative transit velocity

A quantity that can be evaluated without assuming a local velocity field is the cumulative transit velocity

$$U_{\mathrm{cum}}(H) = \frac{H}{\tau(H)}. \tag{15}$$

This quantity is the average axial speed required to traverse the distance H in the residence time; it is not a local Eulerian velocity.

Figure 4 shows $U_{\mathrm{cum}}(H)$ for the four configurations. At 8 m, the main, circular, rectangular and square cases give approximately 8.6 m/s, 5.8 m/s, 8.9 m/s, and 5.9 m/s, respectively. The approximately factor-of-1.5 reduction in cumulative transit velocity for the circular and square configurations relative to the main and rectangular cases is consistent with substantially longer transport paths and/or residence in recirculating regions.

The cumulative velocity also varies strongly with height. This confirms that the residence-time curves cannot be represented as simple plug-flow trajectories with one constant velocity.

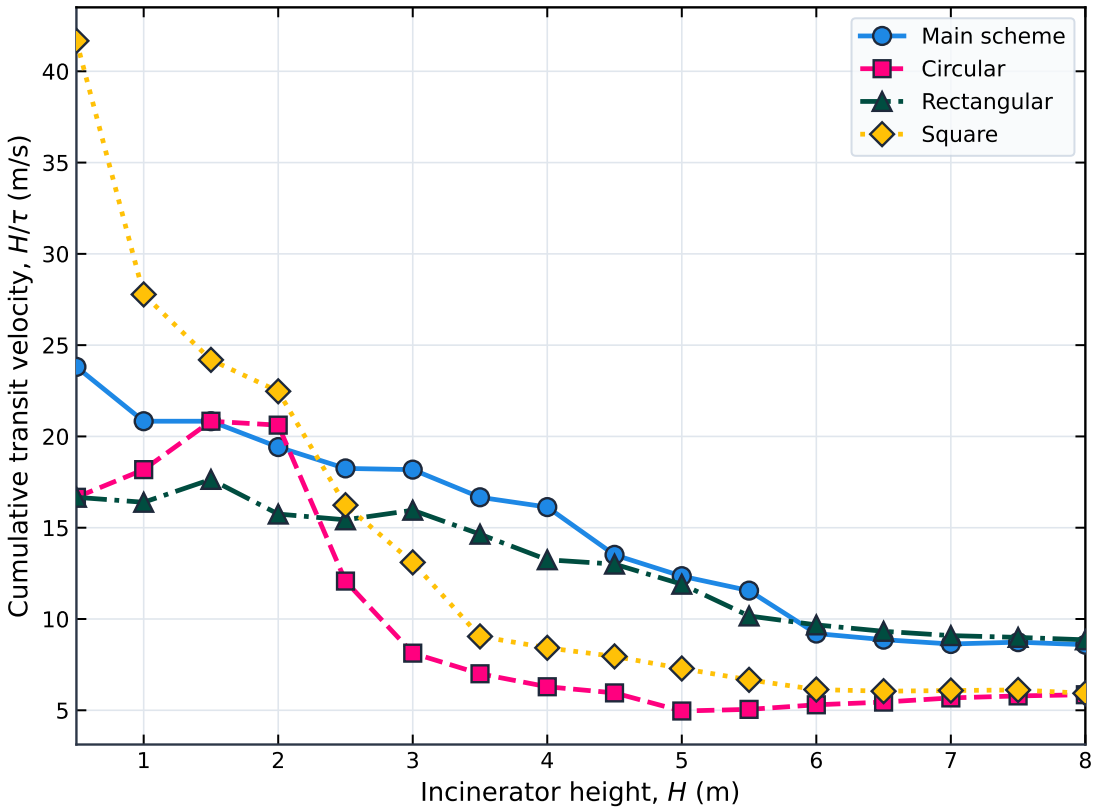

Figure 4: Cumulative transit velocity $U_{\mathrm{cum}} = H/\tau(H)$ reconstructed from the four Darbandi residence-time curves. The quantity is an average velocity over the distance from the inlet reference plane to height H and is not a local Eulerian velocity.

5.3 Constant-velocity diagnostic

For each configuration, a best-fit constant-velocity reference,

$$\tau_{\mathrm{cv}}(H) = \frac{H}{U_{\mathrm{eq}}}, \tag{16}$$

was obtained by least squares over $1 \leq H \leq 8\,\mathrm{m}$. The resulting equivalent velocities and root-mean-square deviations are listed in Table 2.

Table 2: Constant-velocity diagnostic applied to the reconstructed Darbandi data over $1 \leq H \leq 8\,\mathrm{m}$. U_{eq} is an empirical equivalent velocity and is not an independently measured bulk velocity.

Configuration	U_{eq} (m/s)	RMSE (s)
Main scheme	10.06	0.103
Circular	5.94	0.122
Rectangular	10.19	0.078
Square	6.79	0.134

The different U_{eq} values should not be interpreted as four independently measured bulk velocities. They are diagnostic parameters that quantify how much a constant-throughput description would need to change to approximate each curve. The substantially different values for the circular/square and main/rectangular groups demonstrate the geometry dependence of the cumulative transport.

Figure 5 expresses the same result relative to the main configuration:

$$R_j(H) = \frac{\tau_j(H)}{\tau_{\mathrm{main}}(H)}. \tag{17}$$

The circular and square cases increase to approximately 1.47 and 1.45 at 8 m, while the rectangular case remains close to unity.

6 Interpretation of the reduced-order model

The Lambert-W formulation describes one specific mechanism: axial momentum relaxation toward a representative bulk velocity. This mechanism is useful because it has a direct physical interpretation and admits an exact solution. It does not, however, contain radial migration, azimuthal momentum conservation, recirculation-zone trapping, spatially varying mean velocity, or a distribution of Lagrangian path lengths.

The complete Darbandi dataset illustrates the consequence. If the flow were adequately represented by a single axial relaxation process, the four residence-time curves would differ primarily through their

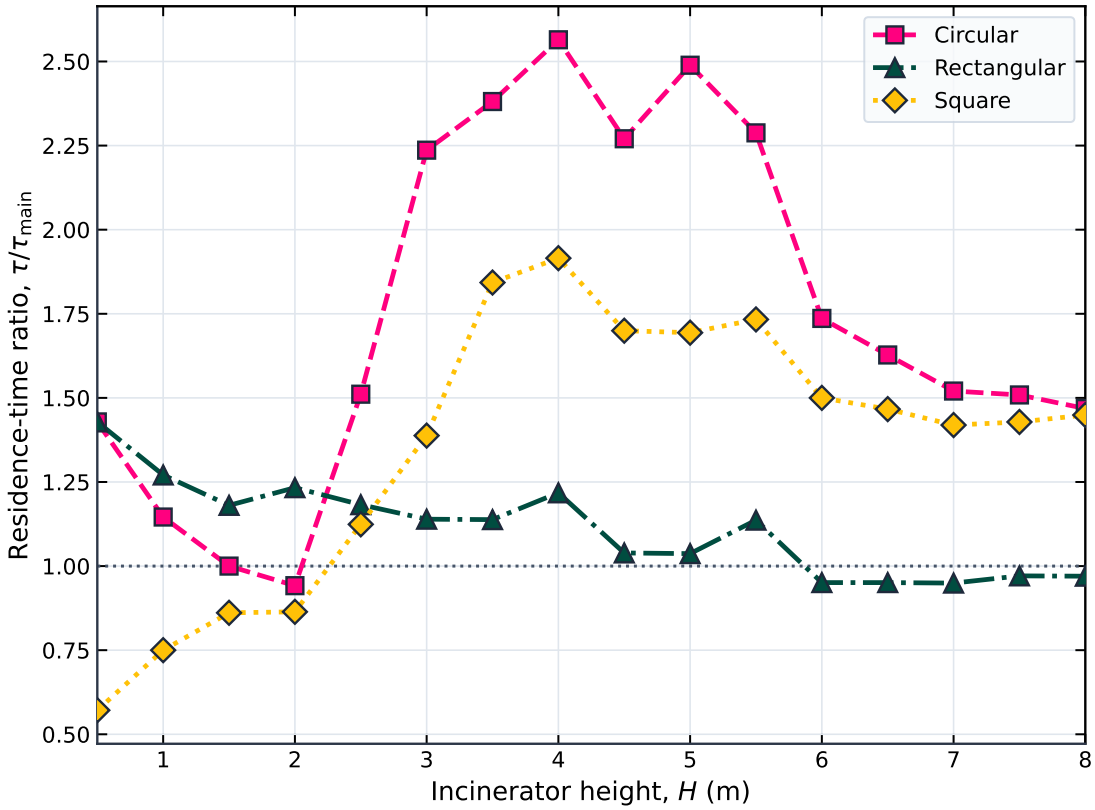

Figure 5: Residence-time ratio relative to the Darbandi main scheme. The geometry-dependent divergence becomes pronounced with increasing height, particularly for the circular and square inlet configurations.

initial axial velocity ratio and relaxation time. Instead, the published curves show geometry-dependent changes in slope that persist over several metres. These changes are naturally interpreted as evidence that the inlet cross-section modifies the three-dimensional flow organization, including the redistribution of waste gas between forward-flowing and recirculating regions.

This interpretation is consistent with the independent literature. Van der Lans et al. [2] measured residence-time distributions in a confined cold swirl flow and represented the system using combinations of plug-flow and continuously stirred regions, specifically to account for several recirculation zones. Doost et al. [3] used LES and experiments to characterize residence-time distributions in a complex swirling combustion chamber and reported a mean residence time of approximately 1.9 s together with non-ideal distribution characteristics. These studies support the use of a distributed-residence-time interpretation rather than a single transit-time description.

The decay of swirl is another relevant physical mechanism. Kitoh [6] showed experimentally that swirl intensity in a turbulent pipe decays downstream and that the velocity field evolves continuously toward fully developed flow. Steenbergen and Voskamp [7] likewise measured the development and decay of turbulent swirling flow and found a Reynolds-number-dependent decay rate. These results indicate that angular momentum cannot generally be represented as a spatially invariant quantity. Consequently, a residence-time model based only on a constant axial relaxation time should be regarded as a first-order baseline.

7 Literature context and cross-study benchmarking

The present formulation is intentionally positioned between a hydraulic transit-time estimate and a full residence-time-distribution calculation. Independent studies provide complementary evidence that swirling reactors can depart substantially from plug-flow behavior and that the numerical prediction of residence time is closely coupled to the quality of the resolved flow field.

Van der Lans et al. [2] measured RTDs experimentally in a cold confined swirl flow using helium tracer measurements at two swirl conditions. Their analysis represented the flow using combinations of plug-flow and continuously stirred regions, explicitly reflecting the presence of multiple recirculation zones. The principal result relevant here is therefore the demonstrated non-ideal shape of the RTD rather than a single scalar residence time.

Doost et al. [3] performed cold-flow LES and experimental characterization of a complex swirling combustor. Their study evaluated the RTD, cumulative distribution, mean, variance and skewness and

reported a mean residence time of approximately 1.9 s. This value is not directly compared with the Darbandi terminal trajectory time because the geometry, operating condition and definition of residence time differ. It is nevertheless an important independent scale for a laboratory swirling combustor.

Mehdizadeh et al. [4] subsequently applied three hybrid URANS/LES approaches to the same general combustor configuration and compared the residence-time characteristics with the LES and experimental reference of Doost et al. Their reported mean residence times for the WALE/LES reference, SST–SAS, SA–IDDES and k–ω–DES cases were approximately 2.07 s, 2.07 s, 2.44 s, and 2.77 s, respectively, as read from their reported residence-time figures. The study concluded that the hybrid methods did not reproduce the residence-time characteristics as well as LES, and linked the discrepancy to differences in the predicted flow field. This result is directly relevant to the present reduced-order framework: residence time is not merely a consequence of total volume and flow rate, but is sensitive to the resolved transport structures.

Arai et al. [5] measured residence-time behavior in a swirl-type combustor using helium tracer measurements. They reported that, when the recirculation zone was tightly established, the residence time was not strongly affected by swirl number; they also found a shorter residence time under hot reacting conditions than under cold conditions. This provides an additional experimental indication that the organization and state of the recirculation zone can matter more than a single inlet swirl parameter.

Kitoh [6] and Steenbergen and Voskamp [7] provide the corresponding flow-mechanics evidence. Kitoh measured exponential downstream decay of swirl intensity in a turbulent pipe, with a decay coefficient that depended on swirl intensity. Steenbergen and Voskamp likewise found that the decay rate depends on Reynolds number and that the initial swirl condition persists over a substantial portion of the decay region. These observations motivate future versions of the present model in which the axial and azimuthal relaxation processes are coupled and spatially varying.

Table 3 and Fig. 6 summarize the numerical residence-time quantities that can be extracted directly from the cited studies without mixing incompatible definitions. The Darbandi values are terminal trajectory times at approximately 8 m; the Doost and Mehdizadeh values are system mean RTDs for a different laboratory combustor. They are therefore shown as contextual benchmarks rather than as a single validation set.

The cross-study comparison therefore reinforces the intended role of the present model. The Lambert-W solution is a transparent trajectory-level baseline; the Darbandi dataset demonstrates strong geometry dependence within one industrial configuration; and the independent RTD studies demonstrate that recirculation and flow-field resolution can substantially alter ensemble residence-time statistics.

Table 3: Residence-time quantities reported or reconstructed from independent swirling-flow studies. The values are not treated as a single commensurate validation dataset because the geometries, operating conditions and residence-time definitions differ.

Study	Method	Residence-time quantity	Reported value
Darbandi et al. [1]	RANS + Lagrangian tracking	$\tau(H = 8\,\mathrm{m})$, main	≈ 0.93 s
Darbandi et al. [1]	RANS + Lagrangian tracking	$\tau(H = 8\,\mathrm{m})$, circular	≈ 1.37 s
Darbandi et al. [1]	RANS + Lagrangian tracking	$\tau(H = 8\,\mathrm{m})$, rectangular	≈ 0.90 s
Darbandi et al. [1]	RANS + Lagrangian tracking	$\tau(H = 8\,\mathrm{m})$, square	≈ 1.35 s
Doost et al. [3]	LES + experiment	Mean RTD	≈ 1.9 s
Mehdizadeh et al. [4]	WALE/LES reference	Mean RTD	≈ 2.07 s
Mehdizadeh et al. [4]	SST–SAS	Mean RTD	≈ 2.07 s
Mehdizadeh et al. [4]	SA–IDDES	Mean RTD	≈ 2.44 s
Mehdizadeh et al. [4]	k–ω–DES	Mean RTD	≈ 2.77 s

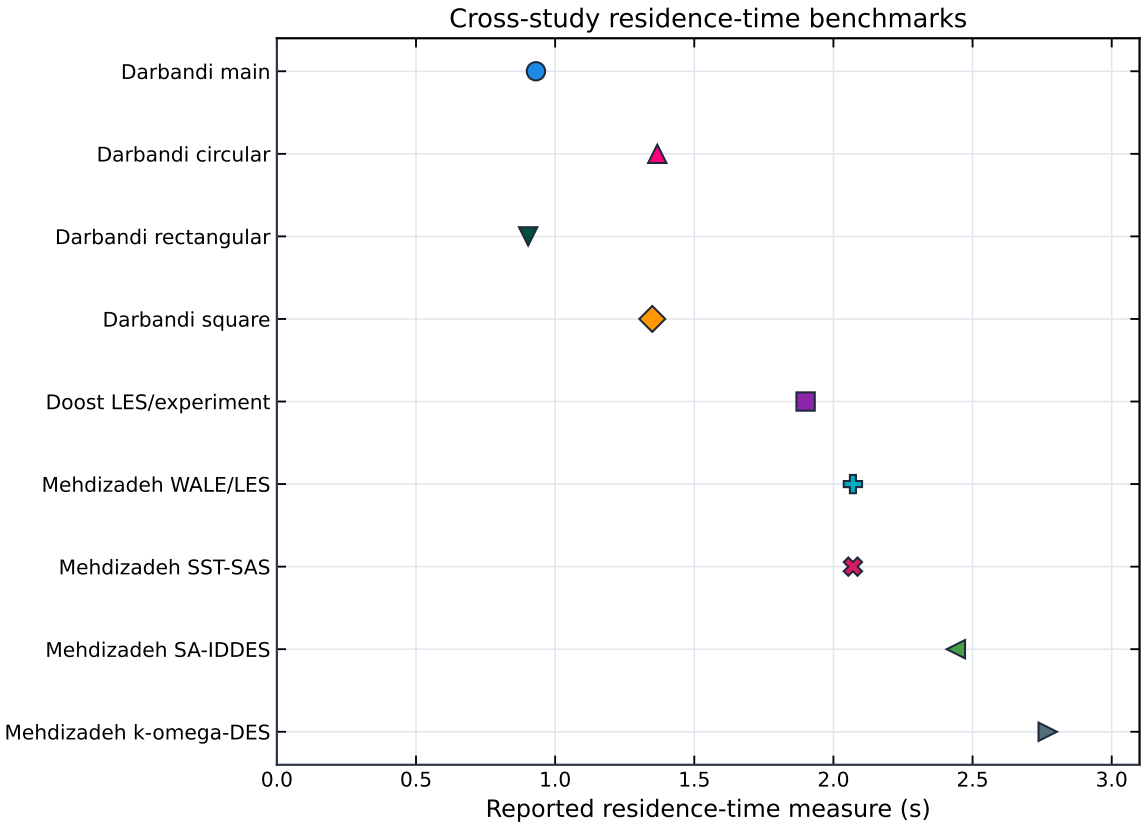

Figure 6: Cross-study residence-time benchmarks. The Darbandi values are terminal trajectory times at approximately 8 m; the Doost and Mehdizadeh values are system mean residence times for a different laboratory combustor. They are therefore shown for physical context rather than as a single commensurate validation dataset.

8 Limitations and extensions

Several limitations should be stated explicitly.

1. The Darbandi residence-time values are reconstructed from a published figure. They are therefore approximate graphical data and not a substitute for the original Lagrangian trajectory database.

2. The present model assumes constant bulk axial velocity. A variable $\bar{w}(z)$ can be retained in the governing equations, but the resulting integral generally does not admit the same simple Lambert-W inversion.

3. Radial and azimuthal momentum are not resolved. This is particularly important for the circular and square configurations, for which the published residence-time curves indicate stronger geometry-dependent transport effects.

4. The parameter T_L is an effective relaxation scale. It should not be interpreted as a directly measured turbulence time scale unless the required local turbulence statistics are available.

5. The residence-time curves in Darbandi et al. are Lagrangian particle-tracking results along the reported computational system. They should not be interpreted as a full outlet RTD $E(t)$ unless the complete ensemble of inlet and exit trajectories is available.

A natural extension is therefore a two-component reduced-order model in which axial momentum and angular momentum evolve simultaneously:

$$\frac{\mathrm{d}w}{\mathrm{d}t} = -\frac{w - \bar{w}(z)}{T_w}, \tag{18}$$

$$\frac{\mathrm{d}v_\theta}{\mathrm{d}t} = -\frac{v_\theta - v_{\theta,\mathrm{eq}}(z)}{T_\theta}, \tag{19}$$

with a geometry-dependent radial redistribution term. Such a model would retain analytical transparency while introducing the minimum additional physics required to represent swirl decay and recirculation.

9 Conclusions

A closed-form residence-time solution based on first-order axial momentum relaxation was derived and expressed exactly using the Lambert-W function. The closed-form analytical solution is governed by two dimensionless quantities, the inlet-to-bulk velocity ratio Θ and the relaxation parameter Λ.

The complete residence-time dataset of Darbandi et al. was reconstructed from the published residence-time figure of Ref. [1] for the main, circular, square and rectangular waste-gas inlet configurations. The analysis shows that the geometry effect is substantial and height-dependent. At approximately 8 m, the reconstructed residence times are about 0.93 s for the main scheme, 1.37 s for the circular inlet, 1.35 s for the square inlet and 0.90 s for the rectangular inlet. Relative to the main configuration, the circular and square cases therefore exhibit approximately 46% and 45% greater residence times, respectively.

The cumulative transit-velocity analysis provides the same physical picture without requiring an assumed local velocity field. At 8 m, the cumulative transit velocities are approximately 8.6 m/s, 5.8 m/s, 5.9 m/s, and 8.9 m/s for the main, circular, square and rectangular configurations, respectively.

In conclusion, the objective of the present work is not to replace CFD, but to isolate the contribution of axial momentum relaxation from the additional transport mechanisms associated with swirl-induced recirculation, three-dimensional redistribution, and geometry-dependent residence-time enhancement. The closed-form Lambert-W formulation provides a mathematically exact baseline for purely axial momentum decay. Deviations from this reference—as observed across the reconstructed inlet configurations—directly quantify the degree to which geometry-dependent three-dimensional flow organization, swirl decay, and recirculation structures dictate the true residence time. Independent experimental and LES literature on confined swirling flows supports the interpretation in terms of recirculation, non-ideal transport and evolving swirl.

The next development should couple axial and azimuthal momentum relaxation and introduce a minimal representation of recirculation-zone residence. Such a model could retain the analytical advantages of the present formulation while directly addressing the geometry-dependent behavior observed in the published CFD benchmark.

Declaration of Competing Interest

The author declares that there are no known competing financial or personal relationships that could have appeared to influence the work reported in this paper.

Data and code availability

The Python scripts used for figure generation and verification are available from the corresponding author upon reasonable request.

Funding

The authors gratefully acknowledge financial support from the Fundação para a Ciência e a Tecnologia, I.P. (FCT), Portugal, which contributed to the support of the research activities underlying this work.

Acknowledgements

This research was funded in whole or in part by the Fundação para a Ciência e a Tecnologia, I.P. (FCT, https://ror.org/00snfqn58) under Grant UIDB/50022/2020 (https://doi.org/10.54499/UIDB/50022/2020), UIDP/50022/2020 (https://doi.org/10.54499/UIDP/50022/2020), LA/P/0079/2020 (https://doi.org/10.54499/LA/P/0079/2020). For the purpose of Open Access, the author has applied a CC-BY public copyright license to any Author's Accepted Manuscript (AAM) version arising from this submission.

References

[1] M. Darbandi, M. R. Modarres, G. E. Schneider, and H. Ghanati, "Cold gas analysis of a waste-gas incinerator to enhance mixing capabilities using CFD," in *Proceedings of the 10th International Conference on Heat Transfer, Fluid Mechanics and Thermodynamics (HEFAT2014)*, Orlando, Florida, 2014, pp. 1177–1184.

[2] R. P. van der Lans, P. Glarborg, K. Dam-Johansen, and P. S. Larsen, "Residence time distributions in a cold, confined swirl flow: Implications for chemical engineering combustion modelling," *Chemical Engineering Science*, vol. 52, no. 16, pp. 2743–2756, 1997, doi:10.1016/S0009-2509(97)00086-9.

[3] A. S. Doost, F. Ries, L. G. Becker, S. Bürkle, S. Wagner, V. Ebert, A. Dreizler, F. di Mare, A. Sadiki, and J. Janicka, "Residence time calculations for complex swirling flow in a combustion chamber using large-eddy simulations," *Chemical Engineering Science*, vol. 156, pp. 97–114, 2016, doi:10.1016/j.ces.2016.09.001.

[4] A. Mehdizadeh, S. Doost, A. Sadiki, J. Janicka, and N. Karimi, "Assessment of predictive capability of hybrid URANS/LES methods in residence time calculation," *Chemical Engineering Science*, vol. 183, pp. 47–59, 2018, doi:10.1016/j.ces.2018.02.035.

[5] M. Arai, T. Nomura, and H. Hiroyasu, "Residence time measurement in a swirl type combustor

with helium tracer," *Transactions of the Japan Society of Mechanical Engineers, Series B*, vol. 53, no. 492, pp. 2619–2625, 1987, doi:10.1299/kikaib.53.2619.

[6] O. Kitoh, "Experimental study of turbulent swirling flow in a straight pipe," *Journal of Fluid Mechanics*, vol. 225, pp. 445–479, 1991, doi:10.1017/S0022112091002124.

[7] W. Steenbergen and J. H. Voskamp, "The rate of decay of swirl in turbulent pipe flow," *Flow Measurement and Instrumentation*, vol. 9, no. 2, pp. 67–78, 1998, doi:10.1016/S0955-5986(98)00016-8.

[8] N. Syred and J. M. Beer, "Combustion in swirling flows: A review," *Combustion and Flame*, vol. 23, no. 2, pp. 143–201, 1974.

[9] R. M. Corless, G. H. Gonnet, D. E. Hare, D. J. Jeffrey, and D. E. Knuth, "On the Lambert *W* function," *Advances in Computational Mathematics*, vol. 5, pp. 329–359, 1996.

[10] B. E. Launder and D. B. Spalding, *Mathematical Models of Turbulence*. London: Academic Press, 1972.